
Design, Fabrication and Performance Evaluation of a Tensile Testing Machine

Michael N. Nwigbo^{1*}, Bright G. Gwarah² and Princewill N. Gwarah³

¹Department of Mechanical Engineering, Kenule Beeson Saro-Wiwa Polytechnic, Bori, Nigeria

²Department of Chemical Engineering, Kenule Beeson Saro-Wiwa Polytechnic, Bori, Nigeria

³Department of Electrical/Electronic Engineering, Kenule Beeson Saro-Wiwa Polytechnic, Bori, Nigeria

*Corresponding Author's Email: nwigbon@yahoo.com

DOI: 10.56201/ijemt.vol.11.no4.2025.pg95.110

Abstract

Tensile testing is an important tool for evaluating fundamental properties of engineering materials, and is critical in developing and controlling the quality of materials, as well as their selection and application in engineering. However, commercial tensile testing machines with the required capabilities are prohibitively not cost effective or user friendly. In addition, they are extremely bulky, so they take up a considerable amount of space and cannot be moved or relocated once they are fixed and calibrated for a position. This study designed and fabricated a single column 200 N, electric powered tensile testing machine, suitable for evaluation of strength properties of non-ferrous metals and their alloys. It was intended to be used for laboratory experiments in Kenule Beeson Saro-Wiwa Polytechnic, Bori. It consists of a mild steel frame, a load cell, lead screw, weighing machine, extensometer, and two bevel gears, with a maximum stroke of 100 mm having vertical motion. The machine is driven by a 1 hp single phase induction stepper motor. The fabricated machine was tested for performance evaluation by conducting tensile test with different aluminium samples. The result revealed an increase in stress value with increased strain, and a linear range at low strain for the sampled aluminium, followed by a transition into a plastic zone up to the breaking point at a strain of 1.5–3.0%. Also, the obtained test results were compared with those from standard commercial tensile testing machine for similar test samples and the error was calculated and found to be less than 10%. The fabricated machine is therefore suitable for evaluation of strength properties of non-ferrous metals and their alloys as well as polymers and composite materials.

Keywords: *Tensile testing, universal testing machine, fabrication, bevel gear, torque, design*

1.0 INTRODUCTION

Materials testing is an essential tool which provides knowledge of the fundamental materials properties, that are critical to their selection and application in engineering design and manufacturing. The most important materials properties for structural applications are the mechanical properties which include strength, hardness, toughness and fatigue among others, which are usually evaluated by means of destructive tests (Yannis and Ioannis, 2017). The tensile testing method is a universally known and acceptable method for evaluating the strength properties of engineering materials, which is achieved with the aid of the tensile testing machine. A tensile test (or tension test) applies force to a material specimen in order to measure the material's response to tensile (or pulling) stress (Muhammad *et al.*, 2023). This type of testing

provides insight into the mechanical properties of a material and enables product designers to make informed decisions about when, where, and how to use a given material. The properties that are directly measured via a tensile test are ultimate tensile strength, maximum elongation and reduction, elastic modulus, Poisson's ratio, yield strength, and strain-hardening characteristics. (Stephen and Vjay, 2020).

Previous studies reveal the importance of efficient and effective materials testing in the production process as it enhances quality assurance, performance optimization, quality control, cost savings, compliance with regulations and safety compliance (Muhammad *et al.*, 2015). Baharuddin and Yani (2018) proposed a vertical type of tensile machine with a maximum load of 5 kN for testing copper and aluminum. The servo motor that drives this tensile testing apparatus has a 100-watt output, and the power is transferred to the device through a V-belt. Cruz *et al.* (2020) also designed and constructed a tensile-compression loading apparatus with a maximum load capacity of 2.5 kN. Even advancements in materials and requirements for the design of micro products call for testing machines with low loads and excellent precision. For example, testing thin workpieces and super-elastic kinds of bio-materials need testing equipment with these characteristics (Gunter *et al.*, 2021; Singh, 2022). However, there has been a tremendous increase in the development of materials of medium-strength, such as composites with a variety of natural or synthetic fiber reinforcement combinations (Rizal *et al.*, 2019; Saidi *et al.*, 2022).

Lim and Kim (2013) developed a miniature tensile tester with a low capacity and intended to pull 6061 aluminum material. They construct horizontal models with a maximum load capacity of 2 kN and a maximum stroke of 20 mm. This system can carry out tensile tests on small tensile specimens at rates ranging from 0.001 to 1.0 mm/s. Rafay *et al.* (2016) designed an automatic tensile testing machine using dual cylinder technique in order to achieve maximum load with the reduction of minimum physical effort to minimize losses. The machine consisted of a servo motor which provides the necessary torque to turn the master cylinder of an incorporated hydraulic actuator. The overall electrical system consisted of a servo motor and driver circuit, an optical encoder, an amplifier, and a controller card. The controller and a PC-bus plug-in interface card connect the computer to the mechanical testing system. The machine was capable of applying a limiting tensile force of 5 kN and operated using hydraulic oil. Test results of machine revealed nonlinearity at approximately 480 MPa with 6% error when compared with conventional tensile testing machine.

Muhammad *et al.* (2015) reported the design and fabrication of a of high temperature creep testing machine for characterization of various materials being used in high temperature applications. Maximum applied load on the specimen can be 10 kN and tests could be carried out at maximum temperature of 700°C. The machine used lever loading mechanism for load application and measures extension up to 55% of gauge length of the specimen. All components were designed and stress analysis was performed. Components were fabricated separately and then assembled. The machine was able to successfully perform tensile creep tests for different materials at various temperatures according to ASTM standard E-139-06. Danladi and Ningi (2022) designed and fabricated a prototype manually operated tensile testing machine using locally sourced materials. The principal parameters used in the design include the maximum load (20 kN), the gage length and diameter of a standard tensile specimen of 50mm and 12.5mm respectively. The major components of the machine include 20-ton hydraulic jack, a locally made axial extensometer and load cell, a fixed and a movable frame. The machine was tested for performance using standard tensile test specimens. The data from the test was used as dummies to demonstrate how to compute the ultimate tensile strength, yield stress, fracture stress, % elongation and %

reduction in area of the mild steel. In another study, Taif *et al.* (2021) designed and fabricated a servo-driven electromechanical high-temperature tensile machine with an integrated environmental chamber. The maximum load capacity was set to be 20 kN with the possibility of future upgrades. The machine was automated by a computerized system that controls the entire operation of the designed machine. The machine was designed to test variety of materials at various temperatures ranging from room temperature up to 500°C. The machine was fully controlled using automated software to control the entire operation and to provide users with a certified test report. The main component consisted of a high-quality aluminum frame that hosts the entire setup, like a furnace, and a universal type gripping mechanism. The structure was monitored by precise measurement instrumentation and a dependable data acquisition system. The machine was validated by testing AA6063-T6 to evaluate the sophistication of the machine's functionality. The results then compared to an international standard, provided close results with a low percentage error of about 4.5% compared to international standard readings.

2.0 MATERIALS AND METHOD

The materials for the fabrication of the tensile testing machine were selected based on the design output. The design analysis adopts a mathematical approach to evaluate the parameters used to determine the performance of the machine as well as materials selection. The parameters considered in this study include maximum torque imposed on the machine, the maximum stress in the load screw, the overall machine efficiency and the lead screw size.

2.1 Maximum Torque

The maximum torque, tension, and buckling forces that occur when the tensile testing machine is subjected to maximum load as designed must be considered in order to ensure the strength of the driving components. The tensile testing machine is intended to support a maximum axial load of 200 N, with a screw lead of 5 mm and an efficiency of 96%. the maximum torque imposed on the load screw was estimated using Equation (1) (Mohammad *et al.*, 2023).

$$T = \frac{F_a p}{2\pi\eta} \quad (1)$$

where, T is the maximum torque imposed on the load screw (Nm), F_a is the maximum axial load (N), p is the screw lead (pitch) (mm), and η is the efficiency of the machine.

2.2 Buckling Load on Machine Frame

The frame of the machine was designed using mild steel bar. There are different types of end connections used in holding frames together. The type of end connection used will affect the performance of the frame. The type of end connection used is the fixed type, because the members are welded together at the ends to give the required rigidity. According to Khurmi and Gupta (2007), the Euler's theory for crippling and buckling load (W_{cr}) under various end conditions is represented by a general equation given by Equation (2).

$$W_{cr} = \frac{C\pi^2 EA}{(l/k)^2} \quad (2)$$

where, C is a constant, representing the end conditions of the column or end fixity coefficient = 4 for welded and bolted joints; E is the modulus of elasticity or young's modulus for the material of the column; A is the area of cross section; l is the length of column and k is the least radius of gyration of the cross section.

The least radius of gyration of the cross section was estimated using Equation (3) (Khurmi and Gupta, 2007).

$$k = \sqrt{\frac{I}{A}} \quad (3)$$

The radius of gyration for known core diameter of screw is taken as $k = 0.25d_c$
And the polar moment of area of the section was obtained as follows

$$I_{XX} = \frac{1}{12}(BD^3 - bd^3) \quad (4)$$

$$I_{YY} = \frac{1}{12}(DB^3 - db^3) \quad (5)$$

$$I = \sqrt{(I_{XX})^2 + (I_{YY})^2} \quad (6)$$

where, D is the outer depth, B is the outer width, b is the inner width, and d is the inner depth.
The area of the column can be obtained from

$$A = (d + B)t \quad (7)$$

2.3 Dimensioning of Machine Frame

The overall dimension of the parts and full structure of the machine was determined considering the specified maximum load to be applied. From the diagram of the frame given in Figure 1(a), for a specified load of 200 N, the total height of the machine was determined using Equation (8).

$$H = a_1 + b + c + a_2 + d + a_3 + e \quad (8)$$

where, a_1 is the width of the structure member; b is the height of the compression tool holder and maximum length of specimen; c is the height of compression arm, a_2 is the width of the cross-steel frame; d is the height of extension arm; a_3 is the width of movable member, and e is the height of the fixed grip.

Considering the diagram in Figure 1(b), the total width of the machine was is determined using Equation (9).

$$W = 2a + b \quad (9)$$

where, a is the thickness of the machine frame and b is the width between frames.

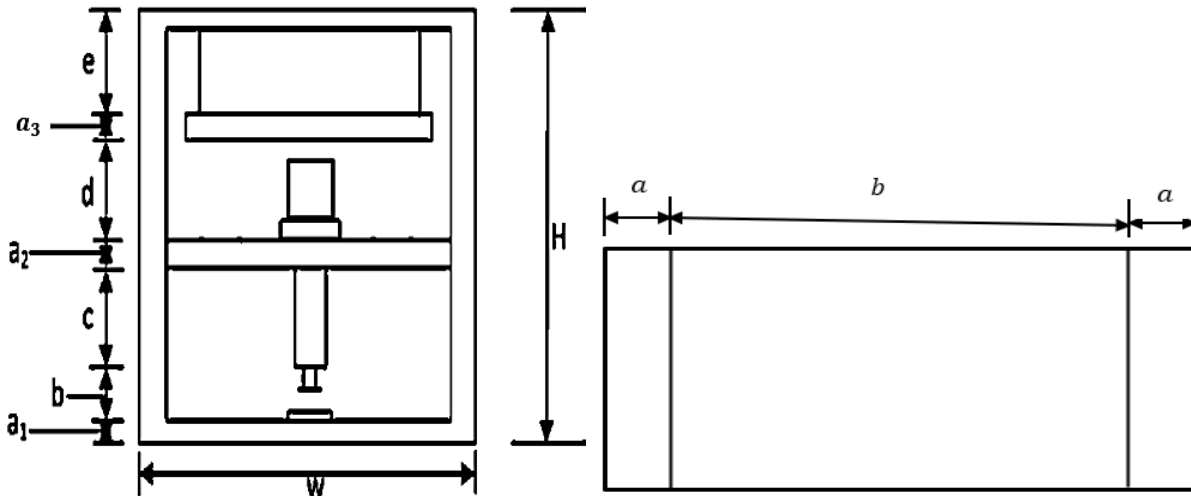


Figure 1: (a) Schematic diagram the machine of frame (b) Schematic diagram the machine width

2.4 Design of the Lead Screw

The machine was designed for the purpose of load a test sample in tension with the total weight of 200 N using a lead screw (Figure 3a). Lead screws are similar to a nut and a bolt in their simplicity

of a simple nut running on a screw. The big difference is that nuts and bolts are used to fasten things together where lead screws are designed for moving things back and forth. The thread of the lead screws is specially designed and optimized for use in linear motion. Since load is transmitted under compression, screw was made from medium carbon steel and also coated with iron with ultimate crushing stress of 320 N/mm^2 , yield stress of 210 N/mm^2 , and shear of 120 N/mm^2 . In compression, the screw was subjected to a load given by Equation (10) (Khurmi and Gupta, 2007).

$$W = \frac{A_s \times \sigma_y}{F.S} \quad (10)$$

where, W is the load, A_s is the area of screw, σ_y is yield stress and $F.S$ is the factor of safety

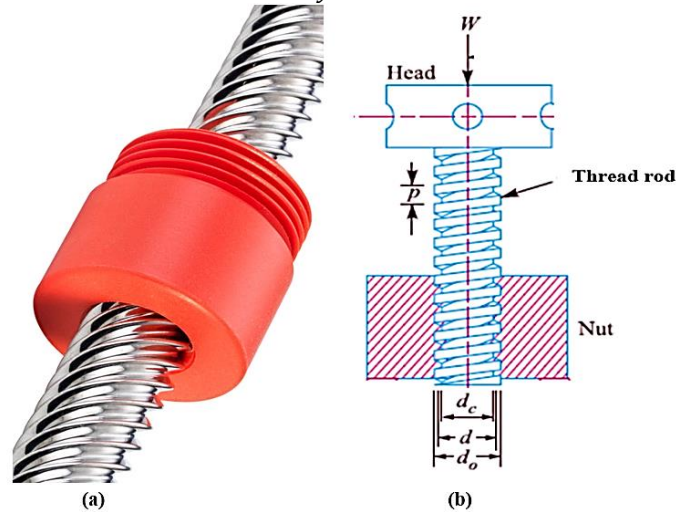


Figure 3: Lead screw geometry and terminology

The design for screw was at the critical load W_{cr} when compressive axial load carried by the screw was just sufficient to initiate buckling. The buckling load on the lead screw was estimated using Equation (11) (Khurmi and Gupta, 2007).

$$W_{cr} = A \times \sigma_y \left[1 - \frac{\sigma_y}{C\pi^2 E} (l/k)^2 \right] \quad (11)$$

where, C is the end fixity coefficient ($= 0.25$); E is the modulus of elasticity or young's modulus for the material of the column; A is the area of cross section; l is the unsupported length of the screw; k is the radius of gyration ($k = 0.25d_c$) and σ_y is the yield stress.

The core diameter of screw was obtained by considering the screw under pure compression using Equation (12) (Khurmi and Gupta, 2007).

$$\sigma_c = \frac{W}{A} = \frac{W}{\frac{\pi d_c^2}{4}} \quad (12)$$

where, σ_c is the compressive stress (Pa), d_c is the core diameter of lead screw (mm), A is the cross sectional area of screw and W is the compressive axial load (N). From this equation, d_c was obtained.

The factor of safety against buckling failure was estimated using Equation (13) (Khurmi and Gupta, 2007).

$$FS_{cr} = \frac{W_{cr}}{W} \quad (13)$$

For safe design of screw under buckling,

$$FS_{cr} > F.S$$

The design for screw was at the critical load (W_{cr}) when tensile axial load carried by the screw was just sufficient to initiate buckling. The Euler's equation of column end buckling given by Equation (14) was used to obtain the length of the lead screw.

$$W_{cr} = \frac{\pi^2 EI}{(l_s)^2} \quad (14)$$

From which the length of the screw was obtained as using (Khurmi and Gupta, 2007),

$$l_s = \sqrt{\frac{\pi^2 EI}{W_{cr}}} \quad (15)$$

where, I is the second moment of area of the screw, E is the elastic modulus and W_{cr} is the crippling load.

2.5 Bevel Gear Design

Bevel gears were used in this study to transmit power from the electric motor to the load screw shaft. Bevel gears are gears where the axes of the two shafts intersect and the tooth-bearing faces of the gears themselves are conically shaped. These gears are most often mounted on shafts that are 90 degrees apart, but can be designed to work at other angles as well, and transmit power at a constant velocity ratio between two shafts. The simplest bevel gear type, the straight tooth bevel gear or straight bevel gear shown in Figure 4 was used in this study. As the name implies, the teeth are cut straight, parallel to the cone axis, like spur gears. These gears are the most economical of the various bevel gear types.

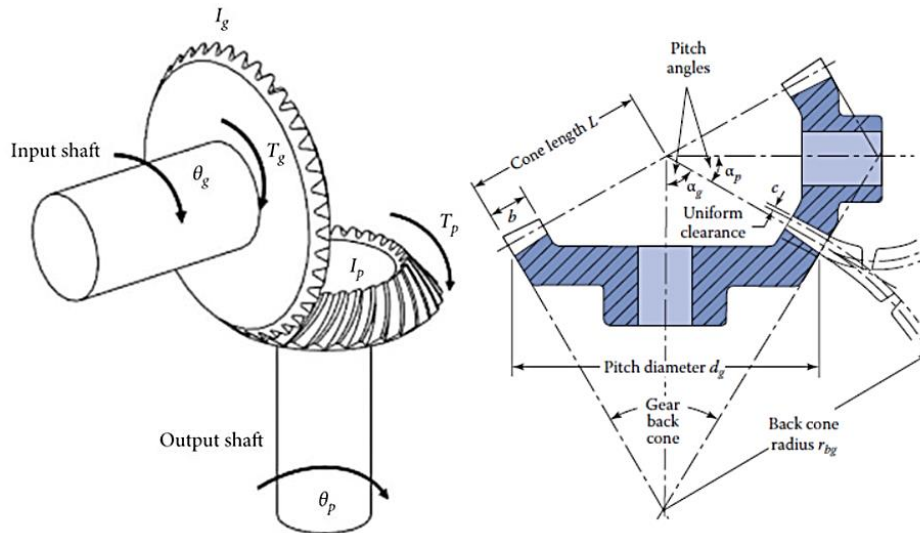


Figure 4: Bevel gears

The transmitted tangential load or tangential component of the applied force, acting at the pitch point P, was calculated using Equation (16) (Khurmi and Gupta, 2007).

$$F_t = \frac{T}{R_{avg}} \quad (16)$$

where, T is the torque applied and R_{avg} is the average pitch radius of the gear under consideration. The torque acting on the pinion was estimated using Equation (17) (Khurmi and Gupta, 2007).

$$T = \frac{60 \times P}{2\pi N_p} \quad (17)$$

where, T is the Power transmitted in watts, and N_p is the speed of the pinion in rpm.

The diameter of the pinion shaft was obtained by using the torsion equation given by (Khurmi and Gupta, 2007)

$$T_e = \frac{\pi\tau(d_p)^3}{16} \quad (18)$$

With $T_e = \sqrt{M^2 + T^2}$ (19)

where, d_p is the diameter of the pinion shaft; T_e is the equivalent twisting moment; τ is the shear stress for the material of the pinion shaft; T is the twisting moment and M is the resultant bending moment.

The speed ratio (velocity ratio) of the gears was estimated using Equation (20) (Khurmi and Gupta, 2007).

$$V.R = \frac{N_p}{N_g} = \frac{T_g}{T_p} \quad (20)$$

where, N_p is the rotational speed of the pinion (rpm), N_g is the rotational speed of the gear (rpm), T_p is the number of teeth on the pinion, and T_g is the number of teeth on the gear.

2.6 Design for Electric Motor Selection

The characteristics of electric motors vary widely with the nature of their application and the type of duty they are expected to perform. For example, the applications like constant speed, constant torque, variable speed, continuous/intermittent duty, steep/sudden starts, frequent start/stops, etc. should be taken into consideration carefully when deciding for the type of a motor for that specific application. The design of an electric motor is therefore, performed to meet certain specifications. The most important among others are the rated power, the rated supply voltage and frequency, the rated speed, and the number of poles. Additionally, the required efficiency and power factor can also be considered as desirable characteristics (Yannis and Ioannis, 2017). However, the motor rated power, torque and speed were considered in this study. The torque produced by the electric motor was obtained using Equation (21) (Khurmi and Gupta, 2007).

$$T = \frac{9550 \times P}{N} \quad (21)$$

where, P is the rated power (kW) and N is the rotational speed of the motor (rpm).

Another important design parameter for electric motor selection is the power rating, which is the power (always the output power in kilowatt or horse power) the motor can deliver without temperature rise exceeding the permissible value. The power rating of the electric motor was obtained using Equation (22) (Khurmi and Gupta, 2007).

$$P = \frac{2\pi TN_p}{60} \quad (22)$$

where, P is the rated power (kW), N is the rotational speed of the motor (rpm) and T is the torque (Nm).

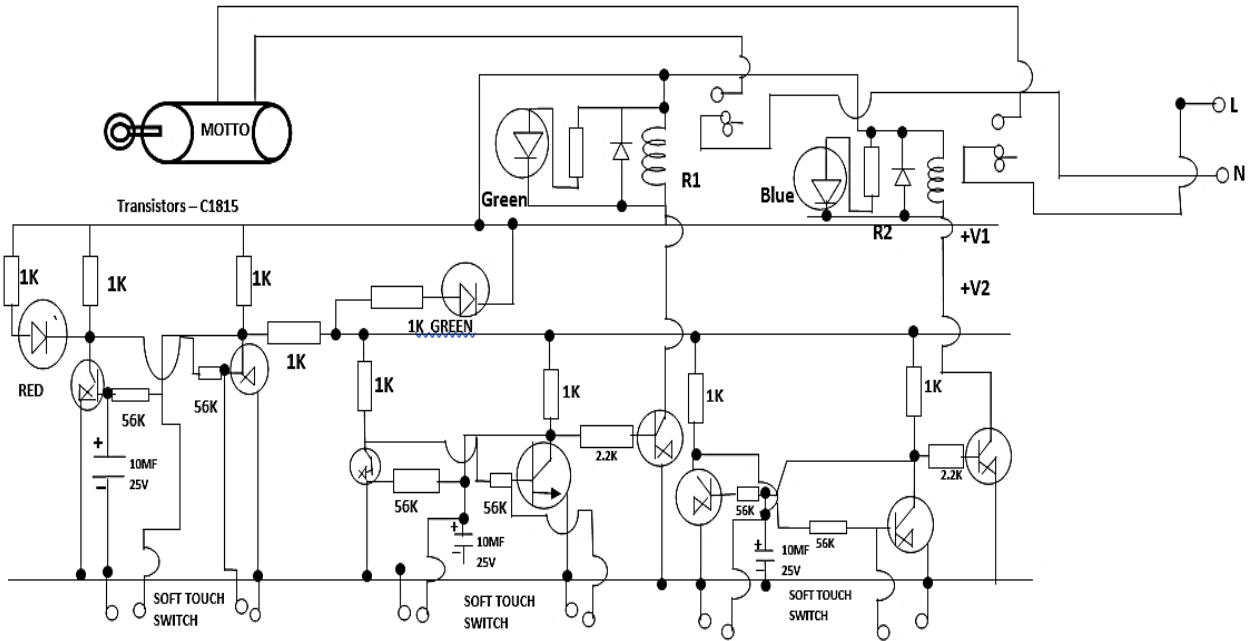


Figure 5: Circuit diagram of the control system: single phase induction motor and forward/reverse switching

Table 1: Design and materials parameters and specifications

S/N	Parameter	Symbol	Value	Unit
1	Load Capacity	P	500	N
2	Maximum stroke	s	100	mm
3	Drive mechanism	Single lead screw and one stepper motor	1.0	Hp
4	Outer width of frame	B	100	mm
5	Outer depth of frame	D	45	mm
6	Inner depth of frame	d	40	mm
7	Inner width of frame	b	90	Mm
8	Thickness of frame	t	5	mm

2.7 Design Calculations

The computations of the various design parameters for the tensile testing machine are presented in Table 2. The computations are based on the equations of the design analysis and design and materials parameters.

Table 3: Design Calculations

Parameter	Input Data	Calculations	Results/Output
Load screw torque	$F_a = 200 \text{ N}; p = 5 \text{ mm};$ $\eta = 0.96; \pi = 3.142$	$T = \frac{F_a p}{2\pi\eta}$	165.79 Nmm
Polar moment of area about XX	$B = 100 \text{ mm}; D = 45 \text{ mm};$ $b = 90 \text{ mm}; d = 40 \text{ mm}$	$I_{XX} = \frac{1}{12}(BD^3 - bd^3)$	279375 mm^4
Polar moment of area about YY	$B = 100 \text{ mm}; D = 45 \text{ mm};$ $b = 90 \text{ mm}; d = 40 \text{ mm}$	$I_{YY} = \frac{1}{12}(DB^3 - db^3)$	1320000 mm^4
Polar moment of area of section	$I_{XX} = 279375 \text{ mm}^4;$ $I_{YY} = 1320000 \text{ mm}^4$	$I = \sqrt{(I_{XX})^2 + (I_{YY})^2}$	1349240.67 mm^4
Area of the column	$B = 100 \text{ mm}; d = 40 \text{ mm};$ $t = 5 \text{ mm}$	$A = (d + B)t$	675 mm^2
Compressive axial load	$A_s = 675 \text{ mm}^2; F.S = 4$ $\sigma_y = 210 \text{ N/mm}^2$	$W = \frac{A_s \times \sigma_y}{F.S}$	35.4 kN
Core diameter of lead screw	$W = 35.4 \text{ kN};$ $\sigma_c = 320 \text{ N/mm}^2$ $\pi = 3.142$	$d_c = \sqrt{\frac{4W}{\pi\sigma_c}}$	11 mm
Radius of gyration	$d_c = 11 \text{ mm}$	$k = 0.25d_c$	2.75 mm
Length of the screw	$W_{cr} = 35.4 \text{ kN}$ $E = 21000 \text{ N/mm}^2$ $\pi = 3.142$ $I = 1349240.67 \text{ mm}^4$	$l_s = \sqrt{\frac{\pi^2 EI}{W_{cr}}}$	2811 mm
Crippling load on machine frame	$A = 675 \text{ mm}^2; C = 0.25;$ $E = 21000 \text{ N/mm}^2;$ $k = 2.75 \text{ mm};$ $l = 2811 \text{ mm};$ $\pi = 3.142$	$W_{cr} = \frac{C\pi^2 EA}{(l/k)^2}$	33.5 N
Torque acting on the pinion	$P = 26 \text{ kW}$ $N_p = 1500 \text{ rpm}$ $\pi = 3.142$	$T = \frac{60 \times P}{2\pi N_p}$	165.5 Nmm
Motor power rating	$T = 165.79 \text{ Nmm}$ $\pi = 3.142$	$P = \frac{2\pi T N_p}{60}$	26 kW

2.8 Materials/Parts Selection

Materials and parts selection are essential aspects of product design and development. Materials selection involves choosing the correct material to suit the requirements of a particular application. This can include design requirements for set manufacturing processes, material attributes such as the chemical, electrical, physical and mechanical property of the material, and the material's cost. The materials used in this study were sourced locally and selected based on their mechanical properties, corrosion resistance, weldability, machinability, availability and affordability. The selected materials were mainly mild steel and stainless steel. The machine frame, load screw, load

cell, grips and fixtures and base stand were fabricated using mild steel, while the gears and other components were fabricated using stainless steel.

2.9 Performance Evaluation of the Fabricated Machine

The fabricated and assembled machine was tested for performance evaluation in the Materials section of the Welding and Fabrication Workshop of the Department of Mechanical Engineering, Kenule Beeson Saro-Wiwa Polytechnic, Bori. The machine was tested by carrying out tensile test on three different samples of aluminium, to measure the following design criteria: tensile strength, yield strength and modulus of elasticity or Young's modulus and ductility with the percentage elongation or percentage reduction in area. The sampled aluminium was first prepared or machined to the standard sample size and shape recommended for tensile and compression testing (Figure 5). The testing procedure is listed as follows.

- (i) A measured length of the sample to be tested was fixed tightly on the specimen holder.
- (ii) The pump was gradually actuated and the load applied to extend the sample was gradually applied.
- (iii) As the load is gradually increased, the material stretches or elongates.
- (iv) The load acting on the material was indicated and read from the pressure gauge, the subsequent elongation was indicated by the extensometer on the stem of the machine.
- (v) The load was continuously increased and the specimen was elongated to its maximum limit to the point of breakage.
- (vi) Three separate tensile tests with aluminium samples were carried out for the aluminium

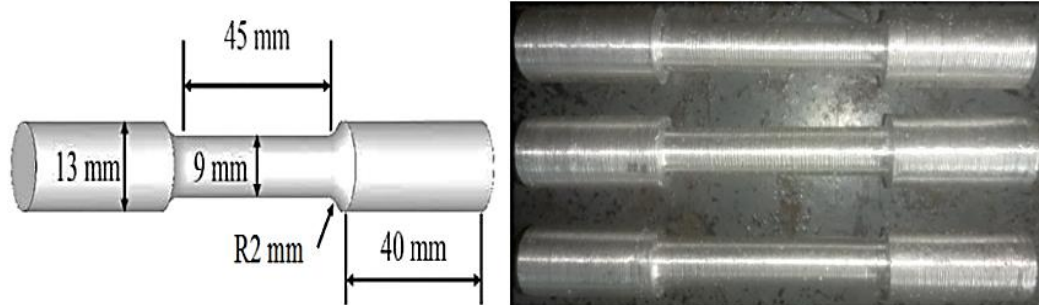


Figure 5: Tensile test samples

2.10 Principle of Operation

As with the standard and other tensile testing machine, the working principle of the designed tensile testing machine involves several key steps:

- (i) **Sample preparation:** The material sample is prepared according to specific standards, which define its dimensions and shape to ensure consistent results (Figure 3.6).
- (ii) **Mounting the sample:** The prepared sample is securely fastened to the machine's grips, ensuring it is aligned properly to avoid any bending stresses during testing.
- (iii) **Applying tension:** The machine applies a tensile force to the sample through the movement of its grips. This force is increased gradually until the sample fails or breaks.
- (iv) **Data collection:** Throughout the test, the load cell sends data to the control system, which records the force applied and the elongation of the sample. This data is then used to calculate the material's tensile strength, modulus of elasticity, and other properties.

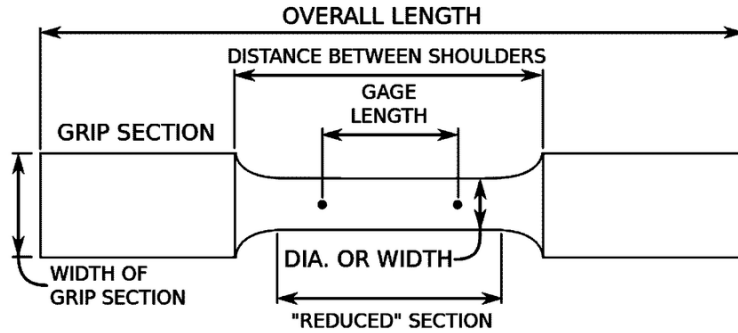


Figure 6: Tensile test specimen and nomenclature

3.0 RESULTS AND DISCUSSION

3.1 Design and Computational Results

After a thorough design analysis and calculations, the result/computational output of the various parameters used in the design and fabrication of the tensile testing machine are presented in Table 1.

Table 1: Design result/computational output

S/N	Design Parameter	Symbol	Value	Unit
1	Load screw torque	T_s	165.79	Nmm
2	Polar moment of area about XX	I_{XX}	279375	mm^4
3	Polar moment of area about YY	I_{YY}	1320000	mm^4
4	Polar moment of area of section	I	1349240.67	mm^4
5	Area of the column	A_c	675	mm^2
6	Compressive axial load	P_c	35.4	kN
7	Core diameter of lead screw	d_c	11	mm
8	Radius of gyration	k	2.75	mm
9	Length of the screw	l_s	2811	mm
10	Crippling load on machine frame	W_{cr}	33.5	N
11	Torque acting on the pinion	T_p	165.5	Nmm
12	Motor power rating	P	26	kW

Table 1 indicates that the theoretical motor power rating of the fabricated 26 kW. However, the selected motor power rating was 1 hp. This is because the designed motor power rating differs significantly from the available standard motor power rating, perhaps due to computational errors or theoretical assumptions. Also, the choice of selection of 1 hp electric motor was due to cost constrain.

3.2 Experimental Results

The test results of the fabricated machine compared with those of a standard tensile testing machine for aluminium sample is presented in Figures 7 and 8. The performance test of the tensile testing machine indicates that it is suitable for obtaining reliable strength properties of ductile materials. The testing phase was completed for elastic deformation of the aluminium specimen by the end of the project timeline.

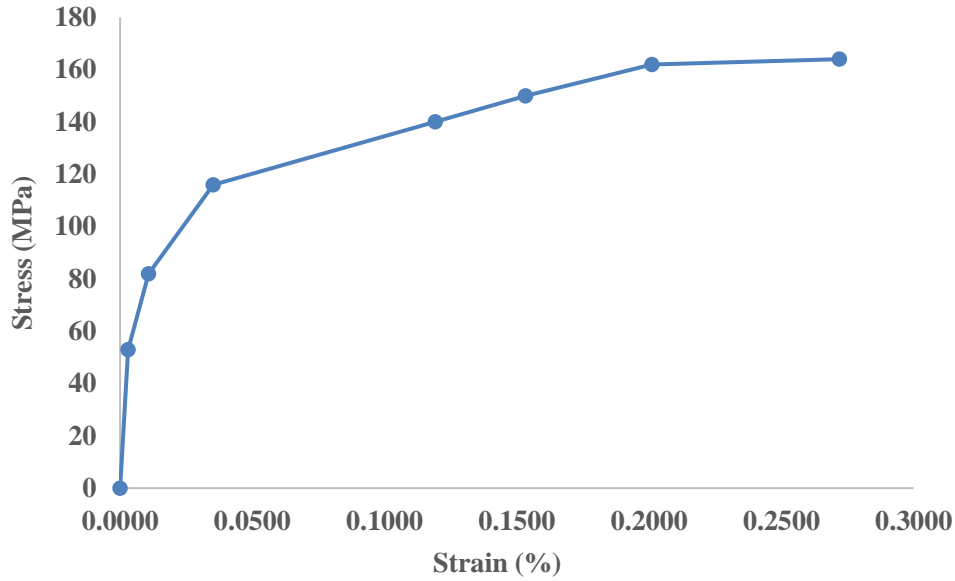


Figure 7: Stress-strain curve for aluminium

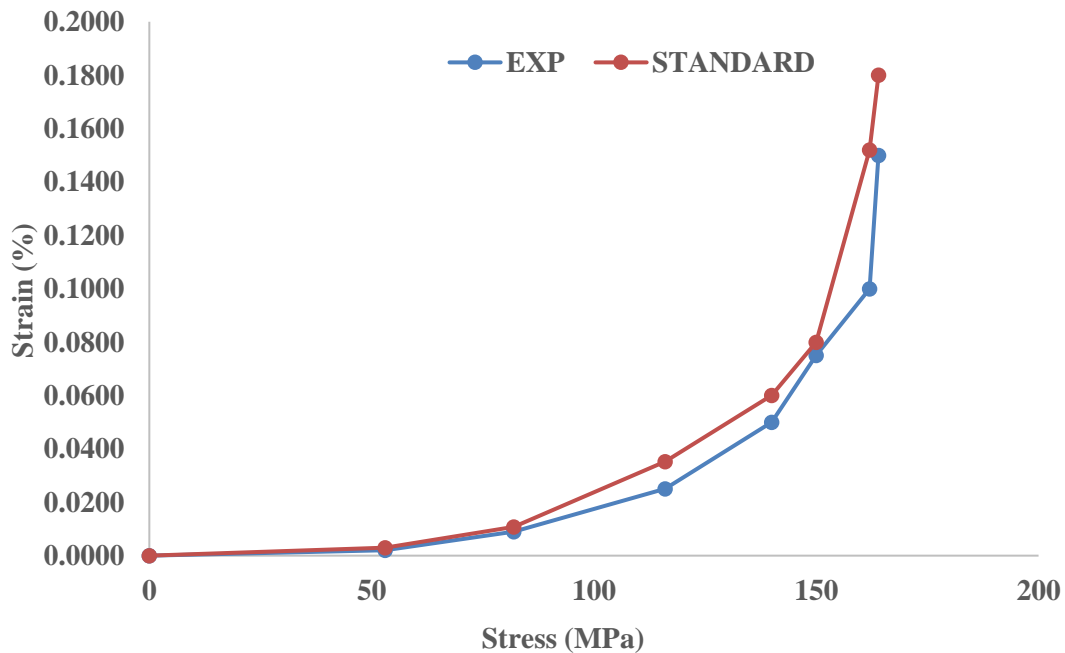


Figure 8: Comparative Strain-stress curve for aluminium

All test curves (Figures 7 and 8) for aluminium show a linear range at low strain, followed by a transition into a plastic zone up to the breaking point at a strain of 1.5–3.0%. Both Figures 7 and 8 indicate that the stress increased with increased strain, for constant experimental parameter. This proves the Hooke's law of elasticity, with elastic modulus being the constant experimental parameter. The fractured test specimens presented in Figure 9 indicate a plastic deformation of aluminium samples. It is evident from the Figure 9 that aluminium has high ductility, hence the fractured surface showed needlelike structures, indicating yielding material fibres. Furthermore, the obtained set of values was compared with the actual standard test values and the error

calculated, found to be 10%. However, the environment temperature, purity of material specimen and other factors could lead to slight deviation and minimizing these factors to controllable extent could increase the machine's performance and optimum results (Danladi, 2022).



Figure 9: Fractured test samples after tensile test

CONCLUSION

The cost-effective tensile testing machine was successfully designed, fabricated and tested for performance by carrying out tensile test with aluminium samples. The machine was easy to operate and maintain, in other to achieve the set objectives. Properties that are directly measured via a tensile test using the machine, include ultimate tensile strength, maximum elongation and reduction in area. The following conclusions were also made:

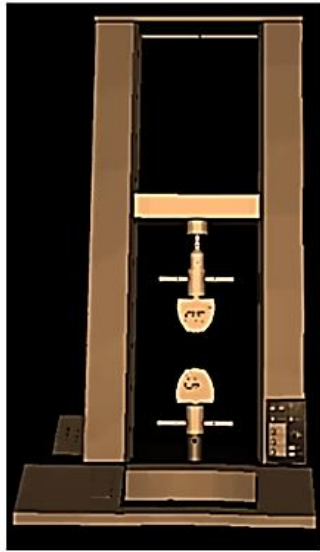
- (i) The tensile testing machine proved to be effective for testing of aluminium and other low melting temperature materials.
- (ii) The obtained stress-strain curves have the same shape as in the case of a standard or commercial tensile testing machine.
- (iii) The absolute error of the comparison test is less than 10%, indicating that the fabricated machine can be used for tensile testing with quite accurate and reliable results

REFERENCES

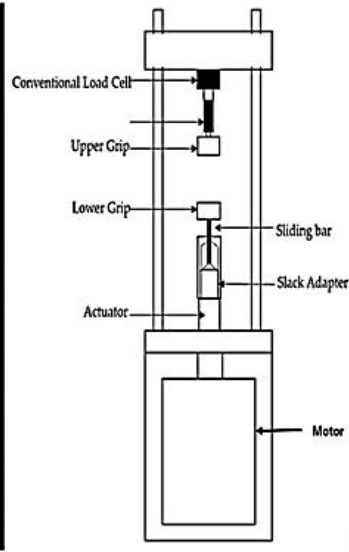
- Baharuddin, K. and Yani, I. (2018). Implementation of design and development tensile testing machine for application in soft material. *Journal of Multidisciplinary Engineering Science and Technology*, 5(12), 9263–9267.
- Cruz, D. J., Shamchi, S. P., Santos, A. D., Amaral, R. L., Tavares, P. J., and Moreira, P. (2020). Development of a mini-tensile approach for sheet metal testing using digital image correlation. *Procedia Structural Integrity*, 25(1), 316–323.
- Danladi, M. D. N. (2022). Design and fabrication of a prototype manually operated tensile testing machine. *International Journal of Advances in Engineering and Management*, 4 (12), 804 – 808.
- Gunter, S. V, Marchenko, E. S., Yasenchuk, Y. F., Baigonakova, G. A., and Volinsky, A. A. (2021). Portable universal tensile testing machine for studying mechanical properties of super-elastic biomaterials. *Engineering Research Express*, 3 (2), 44 – 52.
- Khurmi, R. S. and Gupta, J. K. (2007). *A Textbook of Machine Design*. S. Chand and Company Limited, New Delhi, 1112p.
- Lim, W., and Kim, H. (2013). Design and development of a miniaturised tensile testing machine. *Global Journal of Engineering Education*, 15(1), 48–53.
- Muhammad, R., Udink, A. and Radinal, Y. (2023). Development of a Portable universal testing machine for investigating the mechanical properties of medium-strength materials. *Aceh International Journal of Science and Technology*, 12(1), 25 – 32.
- Muhammad, Z. K., Hassan, S., Adil, M, Aleemullah, F. A. K., Syed, A. A. N., Tak-Hyoung, Lim. and Rak-Hyun, Song. (2015). Design and fabrication of high temperature creep testing machine. *American Journal of Materials Engineering and Technology*, 2015, 3 (3), 51 – 57.
- Rafay, A., Faraz, J., Rafey, I. and Usama, S. S. (2016). Indigenous design for automatic testing of tensile strength using graphical user interface. *MATEC Web of Conferences*, 77 (2016), 1 – 4.
- Rizal, M., Mubarak, A. Z., Razali, A., and Asyraf, M. (2019). Free vibration characteristics of jute fibre reinforced composite for the determination of material properties: Numerical and experimental studies. *AIP Conference Proceedings*, 2187(2), 20 – 32.
- Saidi, T., Hasan, M., & Amalia, Z. (2022). Tensile strength of natural fiber in different types of matrix. *ACEH International Journal of Science and Technology*, 11(2), 136–144.
- Singh, M. (2022). Development of a portable universal testing machine (UTM) compatible with 3D laser confocal microscope for thin materials. *Advances in Industrial and Manufacturing Engineering*, 4 (2), 69 – 76.
- Stephen, J. M. and Vijay, F. (2020). *Development, Validation and Implementation of Universal Testing Machine*. MSc Dissertation, Jönköping University.
- Taif, Y. G., Hussain, J. M. A. and Ahmed, H. R. (2021). Design, fabrication, and testing of an electromechanical high temperature tensile test machine. *Engineering and Technology Journal*, 39 (4), 614-624.
- Yannis, L. K. and Ioannis, D. C. (2017). Design and manufacturing of a single-phase induction motor: A decision aid tool approach. *International Transaction of Electrical Energy System*, 2357 (2017), 1 – 15.

APPENDICES

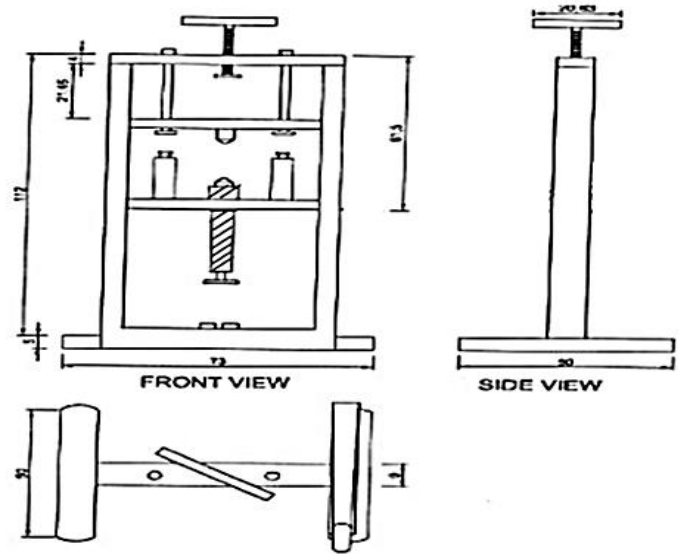
Appendix A: Fabricated tensile testing machine



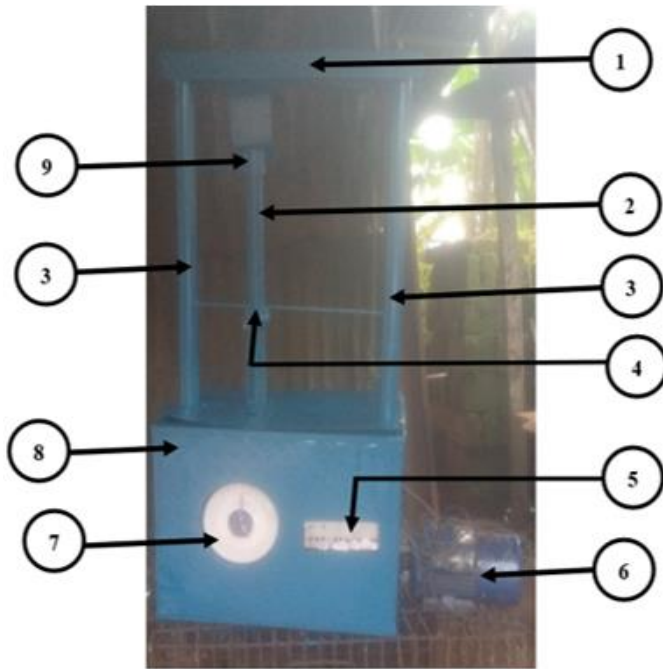
(a) 3D conceptual model



(b) Schematic of the Tensile testing machine



(c) Orthographic view of the tensile testing machine



(d) Pictorial view of the tensile testing machine



(e) Electric motor wiring and fabrication process

Parts list

Item Number	Name	Material	Quantity
1	Frame head (I-beam)	Mild steel	1
2	Load screw	Mild steel	1
3	Frame	Mild steel	2
4	Fixed grip	Mild steel	1
5	Control panel	Polymer	1
6	Electric motor	Cast iron	1
7	Weighing balance	Mild steel	1
8	Housing unit	Mild steel	1
9	Movable grip	Mild steel	1